Theory of dust voids in plasmas

J. Goree,* G. E. Morfill, V. N. Tsytovich,† and S. V. Vladimirov‡
Max Planck Institut für Extraterrestrische Physik, Giessenbachstrasse, 85740 Garching, Germany
(Received 10 December 1998)

Dusty plasmas in a gas discharge often feature a stable void, i.e., a dust-free region inside the dust cloud. This occurs under conditions relevant to both plasma processing discharges and plasma crystal experiments. The void results from a balance of the electrostatic and ion drag forces on a dust particle. The ion drag force is driven by a flow of ions outward from an ionization source and toward the surrounding dust cloud, which has a negative space charge. In equilibrium the force balance for dust particles requires that the boundary with the dust cloud be sharp, provided that the particles are cold and monodispersive. Numerical solutions of the one-dimensional nonlinear fluid equations are carried out including dust charging and dust-neutral collisions, but not ion-neutral collisions. The regions of parameter space that allow stable void equilibria are identified. There is a minimum ionization rate that can sustain a void. Spatial profiles of plasma parameters in the void are reported. In the absence of ion-neutral collisions, the ion flow enters the dust cloud's edge at Mach number $M=1$. Phase diagrams for expanding or contracting voids reveal a stationary point corresponding to a single stable equilibrium void size, provided the ionization rate is constant. Large voids contract and small voids expand until they attain this stationary void size. On the other hand, if the ionization rate is not constant, the void size can oscillate. Results are compared to recent laboratory and microgravity experiments.
[S1063-651X(99)16405-5]

PACS number(s): 52.35.Ra, 52.35.Kt, 52.25.Vy

I. INTRODUCTION

A dusty plasma is an ionized gas containing small particles of solid matter, which acquire a large electric charge by collecting electrons and ions from the plasma [1,2]. A ''void,'' or dust-free region in a dusty plasma, was discovered in several experiments [3–8]. Praburam and Goree [3] found that as particles in a sputtering plasma grew in diameter, an instability developed in two stages. First was the sudden onset of a ''filamentary mode'' of ~100 Hz in which the ionization rate and dust number density were both modulated, and this developed into the second stage, a void. The void was a stable centimeter-size region completely free of dust. Samsonov and Goree [4,5] found that the void has a sharp boundary with the surrounding dusty plasma, as shown in Fig. 1. The electron density and ionization rate were enhanced in the void, compared to the surrounding dust cloud. Melzer, Piel, and Schweigert [7] found a similar void in a silane deposition plasma. Using much larger particles to form a ''strongly coupled'' dusty plasma inside a sounding rocket, Morfill *et al.* [8] observed a centimeter-size void that was usually stable. However, for some operating conditions it exhibited a 1.5-Hz relaxation oscillation, termed the ''heartbeat,'' in which the void shrank drastically and then expanded to its original size. All the experiments described above were carried out in a gas discharge that was sustained by electron-impact ionization, and all featured a void with a sharp boundary.

Two mechanisms are required to explain voids: a force balance on a dust particle, and maintenance of a sharp boundary. The balance of the electrostatic and ion drag forces, as explained by Samonov and Goree [4], involves electron depletion and electron-impact ionization. The term ''electron depletion'' refers to the reduction of electron number density in a dust cloud due to absorption on the particles [9]. This reduces the electron-impact ionization rate in a dust cloud. In a void, the comparatively higher ionization rate leads to an electric field that is directed outward from the void's center. This yields an outward ion flow, which exerts an outward ion drag force on the dust particles, as sketched

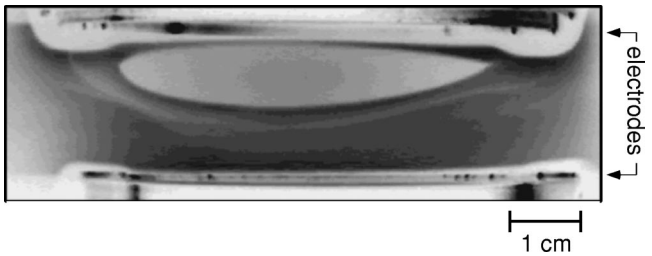

FIG. 1. Image of a void in a carbon sputtering plasma. A dusty plasma is located between the two electrodes. This image is a cross-sectional view, produced by laser light scattering in a vertical plane. Darker grays correspond to higher particle number densities. The particles have a diameter ≈320 nm and a number density $\approx 2\times 10^6$ cm^{-3}. A centimeter-size void appears in the center of the discharge, and in this case it is closer to the powered rf electrode at the top. Note the sharp boundary between the void and the surrounding dust cloud. Reprinted from Samsonov and Goree [4].

*Permanent address: Department of Physics and Astronomy, The University of Iowa, Iowa City, IA 52242. URL: http://dusty.physics.uiowa.edu/~goree. Electronic address: john-goree@uiowa.edu

†Permanent address: General Physics Institute Vavilova 38, Moscow 117942, Russia. Electronic address: tsytov@td.lpi.ac.ru

‡Permanent address: School of Physics, The University of Sydney, Sydney 2006, New South Wales, Australia. URL://www.physics.usyd.edu.au/~vladimi.
Electronic address: S.Vladimirov@physics.usyd.edu.au

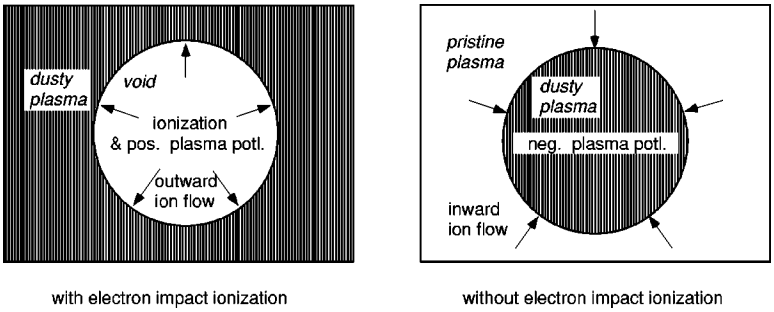

FIG. 2. Sketch of a void (left) and its converse (right). In the presence of electron-impact ionization, a positive space potential develops, creating an outward ambipolar electric field that drives ions outward, applying an outward ion drag force, which can maintain a void. In the absence of electron-impact ionization, for example in a space plasma where plasma is generated far away, the dust cloud forms in the complementary shape of a spheroid, with its boundary sustained by an inward ion drag force driven by an inward electric field.

in Fig. 2. In equilibrium, there is a balance of forces on a dust particle: an inward electrostatic force and an outward ion drag force.

''Ion drag'' is the force exerted on a charged dust particle by flowing ions. It arises from two mechanisms: some ion orbits are deflected by the Coulomb attraction of a negatively charged dust particle, exerting the ''orbit force,'' while others strike the particle surface, exerting the ''collection force'' [10]. (These forces were called the ''Coulomb collision'' and ''charging collision'' forces, respectively, in the review by Tsytovich [2].) The collection force increases with the ion velocity, whereas the orbit force has a peak at the ion thermal velocity, as shown in Fig. 3. When $T_i/T_e \ll 1$, there are three regimes for the ion drag force: subthermal, intermediate, and supersonic. The latter is due solely to the collection force. In this paper we will use approximations for the ion drag force that are valid in the intermediate and supersonic regimes.

The second mechanism required to explain the voids is the maintenance of a sharp boundary. Sharp boundaries are a common feature of dusty plasmas, not only those with voids,

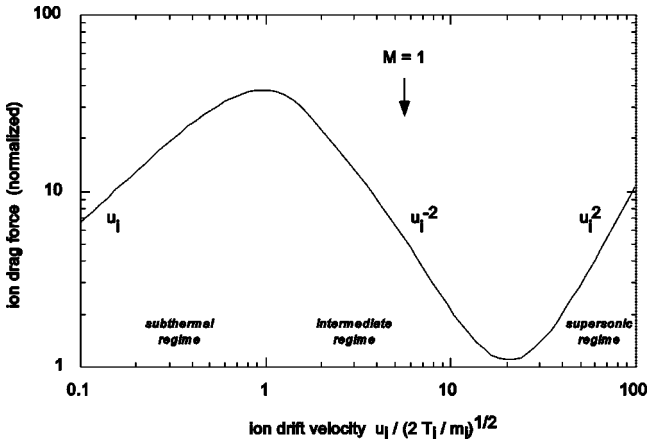

FIG. 3. Ion drag force dependence on ion drift velocity. There are three regimes, corresponding roughly to subthermal and supersonic ion velocities, with an intermediate regime between. The power-law scaling with ion velocity u_i is indicated for these three regimes. The ion velocity is normalized by $\sqrt{2T_i/m_i}$, and the ion drag is normalized by the force $4\pi n_i a^2 T_e/\sqrt{T_i/T_e}$. The plasma parameters assumed are $T_e=3$ eV, $T_i=0.05$ eV, and $n_e=n_i=10^{10}$ cm^{-3}; the particle radius $a=0.1$ μm; and the floating potential is $z=2.7$ in units of T_e, corresponding approximately to the experiments of Refs. [4–6].

but many others as well. In the laboratory, dome- and ring-shaped dust clouds form above electrodes in etching plasmas, and these clouds have a sharp edge [11]. Planetary rings [2,13] and the noctilucent clouds in the lower ionosphere [12] also have sharp boundaries. In a theoretical model of a dust cloud surrounded by a clean plasma, Tsytovich [15] found that the existence of a numerical solution of the hydrodynamic equations required a sharp boundary. This resolved a problem that had arisen in a previous attempt [14] to model a stationary interface between a dust cloud and a clean plasma [16]. In the present paper we will extend the method of Ref. [15] by including ionization and superthermal plasma fluxes, which are required to explain the voids. We develop the boundary conditions required to solve the void problem with a sharp boundary.

In experiments [4,5], the void arises from a uniform dust cloud as a result of an instability. This instability develops as follows. Suppose that in a uniform dust cloud in a gas discharge, there is a spontaneous fluctuation in the dust number density. In the region of reduced dust density, there is less electron depletion by the dust. This leads to a higher electron density there, and a correspondingly higher ionization rate. This ionization hot spot will develop a positive space charge with respect to the surrounding medium. The resulting outward electric field applies two forces to the negatively charged dust particles: an inward electrostatic force and an outward ion drag force Fig. (2). For a small particle size, the inward force will dominate and fill the hot spot again with dust, and the fluctuation will disappear. This is the initial stable situation. However, if the particle exceeds a critical size, the outward ion drag force exceeds the electrostatic force. The region of reduced dust density will then expel more dust particles, and the fluctuation will grow. This is an instability that yields the ''filamentary mode.'' The threshold for the instability is determined by particle size and electric field strength. The particle size is an independent parameter, whereas the electric field is determined self-consistently by the electron and ion transport mechanisms and Poisson's equation. This initial stage of linear growth was modeled by D'Angelo [17].

After sufficient growth, the mode becomes nonlinear, and the growth saturates. This final nonlinear state cannot of course be predicted by a linear model of the instability. One possible final state, as seen in some experiments [3–6], is a stable void.

In this paper we model stable equilibrium voids. The history that led to the formation of the void, whether by an instability as described above or by some other mechanism, is not modeled here. Because the equilibrium develops through nonlinear effects, we use a nonlinear treatment of the relevant fluid equations. The only collisions taken into account are dust-electron and dust-ion collisions inside the dust region. We use this model to predict the conditions for a void's existence, its size, and its sharp boundary with the surrounding plasma.

We scanned a broad range of plasma and dust parameters to map out the phase diagram for void size. This diagram is useful to show that the void is a stable equilibrium and to determine the range of parameters where voids can exist. We show that if a void can appear, there is usually one stable void size, and we find the characteristic time of the evolution to that size.

The void's existence requires a local source of ionization of a background gas. This means that the problem we investigate here is mainly applicable to gas discharges, where the ionization is due to electron impact, although photoionization and other sources of ionization could have a similar effect. In the absence of local ionization, the converse of a void appears, as sketched in Fig. 2. This latter problem is applicable for example to astrophysical dust clouds, and it was modeled by Tsytovich [2]. Electron depletion in the dust cloud causes the dust cloud to acquire a negative space charge, which attracts ions. In the absence of ionization, the ions must originate from a distant plasma source. Thus there is an inward ion flow that creates an inward ion drag force. This collapses the dust cloud into a compact shape, whose size is regulated by a balance of the outward electrostatic force and the inward ion drag force. This problem is analogous to the void problem we treat here, except that by including a local ionization source, the ion flow causes a void to develop.

II. MODEL

A. Overview

We develop a one-dimensional model based on a set of fluid equations, Poisson's equation, and a charging equation for dust. These equations are nonlinear, and we solve them numerically.

We assume equilibrium conditions where all time derivatives are zero. This equilibrium assumption is appropriate both for steady-state conditions and for a void that develops so slowly that an electrostatic equilibrium is always maintained. This assumption also implies that electron-ion pairs are ultimately absorbed by dust or a wall located beyond the dust region. We do not need to extend our simulation volume that far, however, since solving the void problem requires only that we find the dust cloud parameters at the void's boundary.

In the model, all variables depend only on the distance x, as sketched in Fig. 4. We suppose that the problem is symmetric around $x=0$, which is the system's center. The electric potential and ion drift velocity are zero at the center. If the void appears, its center is at $x=0$. Thus we model two regions: the void with $|x|<x_v$, and the surrounding dusty plasma with $|x|>x_v$, where x_v indicates the void boundary.

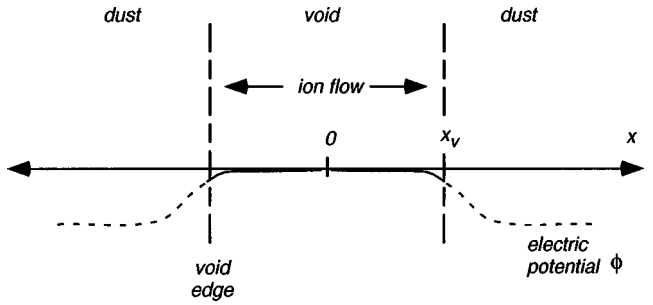

FIG. 4. Sketch of the one-dimensional simulation configuration. A dust cloud fills all space except for a void region of full width $2x_v$ centered at $x=0$. The boundary conditions are $\phi \propto x^2$ near the origin and $\partial\phi/\partial x$ continuous at $x=x_v$. The numerical solutions we will present are valid for the void region $x \leqslant x_v$.

We will develop equations that are valid in both the void and the dust regions. We will solve the equations numerically in the void region, using the equations in the dust region to specify the boundary conditions at the void's edge. Our numerical results will therefore be valid for $|x| \leqslant x_v$.

Dust grains are charged negatively due to the large ratio of the electron and ion thermal velocities. Three forces act on the dust: electrostatic, ion drag, and neutral gas drag. The latter force is proportional to the dust particle velocity, which is zero in the stationary state, but we retain it to include the void velocity during slow motions. The ions are subject to the electrostatic force, while the electrons are Boltzmann distributed. We neglect ion-neutral collisions.

In many ways, the problem we solve resembles a sheath [18,19]. The void region bounded by a dust cloud is analogous to a plasma bounded by an electrode sheath. The difference is the boundary condition for a void is different and more complicated. An electrode sheath develops in front of an electrode, which is at a fixed position and absorbs electrons and ions at its surface. In contrast, the boundary of a dust cloud can move freely in response to forces on the dust, and it is a diffuse body penetrated by electrons and ions. We must model the interior of the dust cloud in order to predict where its boundary will be, and at what potential.

B. Dimensionless variables

The dimensionless variables that we will use are defined here. Dimensionless quantities appear on the left-hand-side of the equations below.

The ion and electron densities are normalized by the ion density n_{0i} at the center $x=0$,

$$n \equiv n_i / n_{0i},$$

$$n_e \equiv n_e / n_{0i}.$$

The temperature ratio is

$$\tau \equiv T_i / T_e.$$

The electric potential is normalized by the electron temperature,

$$\psi \equiv e\phi / T_e.$$

The most convenient normalizations for the electric field and position will be

$$E \equiv \frac{e d_i^2}{a T_e \sqrt{T_i/T_e}} E, \tag{1}$$

$$x \equiv \frac{a \sqrt{T_i/T_e}}{d_i^2} x, \tag{2}$$

where a is the dust particle radius. The ion Debye length d_i is approximated as $d_i = (T_i/4\pi n_{0i} e^2)^{1/2}$. If the effect of streaming ions were taken into account, d_i would be larger [20]. The dimensionless potential ψ and the electric field are related by

$$E = -\frac{\partial \psi}{\partial x}. \tag{3}$$

The two important velocities in the problem are the ion velocity u_i with respect to the dust, and the dust velocity v_d with respect to the neutral gas. These velocities are vastly different in magnitude, and they are not determined by the same forces. Thus it will prove convenient to adopt different normalizations for them. The ion drift velocity u_i is normalized using the ion thermal velocity $v_{Ti} = (T_i/m_i)^{1/2}$,

$$u \equiv u_i / \sqrt{2}\, v_{Ti},$$

or as a Mach number

$$M \equiv u_i / \sqrt{T_e/m_i}.$$

The dust velocity v_d is normalized by several factors including the thermal velocity of the neutral gas, $v_{Tn} = (T_n/m_n)^{1/2}$,

$$v \equiv \frac{v_d}{v_{Tn}} \frac{n_n}{n_{0i}} \left(\frac{3T_n}{T_e} \right) \sqrt{\tau}, \tag{4}$$

where n_n is the neutral gas density.

In the regions where there is dust, we will need additional dimensionless parameters. In physical units, the negative dust charge is $-eZ_d$, where $e>0$ and $Z_d>0$. The dimensionless dust charge and dust number density parameter P are

$$z \equiv Z_d e^2 / a T_e, \tag{5}$$

$$P \equiv n_d Z_d / n_{0i}. \tag{6}$$

The dimensionless charge z is equivalent to the grain's floating potential $-Z_d e/a$ normalized by T_e. Its value, which must be computed from a charging equation, is typically $z \approx 2.5$. The dust number density parameter P in Eq. (6) is essentially the ratio of the negative charge density of the dust compared to that of the electrons in a clean plasma. Our parameter P is defined, as in Refs. [14,15], in a way that is useful for our nonlinear problem. It is related to the parameter introduced in Ref. [9] by $P_{\text{Havnes}} = P n_{0i}/(n_e z)$. When $P \sim 1$, the electrons in the dusty plasma are substantially depleted.

A few more dimensionless parameters will be defined later. These include the ionization rate and, in the dust region, the ion drag force and the dust charging rate. For the problem of expanding and contracting voids, we will also require a normalization for time.

C. Simplifying approximations

In this section we list the approximations. Our model is one dimensional. This is adequate for predicting the existence of a stable void equilibrium and the size of a void, but we cannot predict the three-dimensional shape of a void, as shown in Fig. 1.

The dust particles are assumed to be spherical and monodispersive, and they emit no electrons. The latter assumption is appropriate for laboratory experiments, but not for astrophysical conditions where photoemission and secondary emission often result in a positive dust charge. Gravity, which would be a factor for laboratory experiments with particle sizes >1 μm, is neglected since the void experiments to date either had smaller particles [4] or were carried out under microgravity conditions [8]. Our fluid model neglects dust inertia effects which would play a role at the dust cloud's boundary; these are unimportant for small dust particles and in a stationary equilibrium.

We neglect dust kinetic effects, which might play a role at the dust cloud's boundary. We neglect any heat transfer processes, which might influence the void movement and formation.

By assuming equilibrium conditions, we are unable to model fast-moving voids, which have not been reported in experiments anyway. We will present equations useful for any kind of slow motion of a void. While several kinds of void motion are possible, in our numerical solutions we will evaluate only one kind: expansion and contraction about a stationary center.

We approximate that T_e and T_i are spatially uniform, with the same values in the void and the dust. It is known from simulations [21] of dusty gas discharges that T_e is higher in the dust cloud by as much as a factor of 2. We do not account for this; if we did, it would likely affect our results quantitatively but not qualitatively. We also neglect ionization in the dust region, since it was shown in the experiments [4] to be severely depressed there, as compared to the void. We use an approximate expression for the ion Debye length that neglects the streaming ions, as explained above. The Coulomb logarithm for ion scattering by dust will be affected by the latter approximation. This can affect the ion drag force by as much as a factor of 2, since the logarithm typically has a small value for this problem.

Perhaps the most noteworthy approximation is that we do not include ion-neutral collisions, which would exert a drag force on the ions. They reduce the ion velocity, which affects the ion drag force on a dust particle as well as the dust particle's charge.

In computing the ion drag force on the dust particles, we assume the ion velocity in the dust region is superthermal. We require only that this assumption be valid at the boundary between the dust and void, and our results show this is always true for our plasma conditions without ion-neutral collisions. The drift of electrons is neglected, since it is assumed to be slow compared to the electron thermal velocity.

D. Equations in the void region

In the void region there is no dust, so we include only the electrons and ions in Poisson's equation. All equations are for a steady state, with $\partial/\partial t=0$.

With normalization of Eq. (2), Poisson's equation inside the void is

$$\frac{\partial E}{\partial x}=\left(\frac{d_i}{a}\right)^2(n-n_e). \tag{7}$$

We assume that the electrons are Boltzmann distributed, $n_e=n_{0e}\exp(\psi)$, so that

$$\frac{1}{n_e}\frac{\partial n_e}{\partial x}=\frac{\partial \psi}{\partial x}. \tag{8}$$

The left- and right-hand sides of Eq. (8) correspond to the electron pressure force and the electrostatic force, respectively, which balance each other in equilibrium.

The ion momentum equation also expresses a force balance in equilibrium. The expression in physical units,

$$u_i\frac{\partial u_i}{\partial x}=-\frac{e}{m_i}\frac{\partial \phi}{\partial x}, \tag{9}$$

can be integrated and rewritten in dimensionless units as

$$\tau u^2=-\psi, \tag{10}$$

which is equivalent to conservation of energy for ion motion in the absence of collisions. We neglect ion-neutral collisions, which would apply a drag force on the right-hand side of Eq. (9).

The ion continuity equation

$$\frac{\partial n u_i}{\partial x}=\nu_i n_e$$

includes the ionization source on the right-hand side. Here ν_i is the plasma ionization frequency, which increases exponentially with T_e and also depends on the atomic parameters of the neutral gas [22]. Since we assume T_e is uniform, ν_i will be uniform as well. For simplicity, we will neglect ionization in the dust cloud, since an experiment [4] showed that ionization is highly suppressed in the dust, due to electron depletion. We will also approximate that the ionization rate is uniform in the void, since it will turn out that n_e is fairly uniform inside the void. Thus we approximate

$$\frac{\partial n u}{\partial x}=\begin{cases}\nu_i n_{0e} & \text{if } |x|<x_v\\ 0 & \text{if } |x|>x_v\,.\end{cases}$$

Rewriting the ion continuity equation in dimensionless units, we have

$$\frac{\partial n u}{\partial x}=\begin{cases}1/x_{0i} & \text{if } |x|<x_v\\ 0 & \text{if } |x|>x_v\,,\end{cases} \tag{11}$$

where

$$1/x_{0i}\equiv\frac{n_{0e}\nu_i d_i^2}{n_{0i}a\,v_{Ti}\sqrt{2T_i/T_e}} \tag{12}$$

is the dimensionless ionization rate.

Boundary conditions are required at the center $x=0$ and at the void's edge. At the center, symmetry requires that $E=0$, so that the potential is parabolic for small x:

$$\psi|_{x\to 0}\propto x^2. \tag{13}$$

This is the first boundary condition to be satisfied. Further boundary conditions will be applied at the void's edge, $x=x_v$.

E. Equations in the dust region

In the region occupied by dust, the dust charge should be taken into account in Poisson's equation. This requires finding the self-consistent dust charge and number density. The charge is found from a charging equation, which depends on the electron and ion parameters. The number density is found using the equations of motion and continuity for dust. First we give Poisson's equation, then equations for the dust, and finally equations for the electrons and ions.

Poisson's equation in dimensionless units is

$$\frac{\partial E}{\partial x}=\left(\frac{d_i}{a}\right)^2(n-n_e-P). \tag{14}$$

An exact analytic solution of Poisson's equation in the dust region is possible because of the electrostatic force balance for dust particles. Under our assumption of steady-state conditions we neglect dust inertia, so that the force balance on a dust particle, in physical units, is

$$F_E+F_{\rm dr}+F_{\rm fr}=0, \tag{15}$$

where the Coulomb, ion drag, and neutral drag forces are, respectively,

$$F_E=-Z_d eE,$$

$$F_{\rm dr}=m_i u_i \nu,$$

$$F_{\rm fr}=3n_n a^2 v_{Tn} m_n v_d\,.$$

Here ν is the collision frequency for momentum transfer between ions and dust, and the expression given for $F_{\rm fr}$ is for diffuse reflection from a sphere [23,24]. The electric field appearing in Eq. (15) includes the field of the dust particles. In dimensionless form, Eq. (15) is

$$-zE+unz^2\alpha_{\rm dr}=v, \tag{16}$$

where the first and second terms on the left-hand side correspond to the electrostatic force and the ion drag force, respectively, and the right-hand side is the friction force with the neutral gas. For a stationary void, where the dust velocity v is zero, the force balance is simplified as

$$-E+unz\alpha_{\rm dr}=0. \tag{17}$$

In Eqs. (16) and (17) we have introduced a dimensionless coefficient $\alpha_{\rm dr}$ for the ion drag:

$$\alpha_{\rm dr}=\frac{\tau^{3/2}}{4\pi n_i a^2 v_{Ti} z^2}\,\nu.$$

Writing out ν, the ion drag collision frequency [10], the coefficient is

$$\alpha_{\rm dr}=\frac{1}{2\sqrt{\tau}\,u^3}\left[\ln\left(\frac{d_i}{a}\right)+\frac{\tau u^2}{z}+\frac{\tau^2 u^4}{z^2}\right], \tag{18}$$

where the first term in brackets corresponds to the orbit force, while the last two terms correspond to the collection force. There are several approximations in this expression, which we list here. The Coulomb logarithm in the orbit force corresponds to an integral over ion impact parameters ranging from a minimum of the particle radius to a maximum of the ion Debye length. The true minimum impact parameter is actually larger than a because of the attractive potential of the negative dust particle [10]. The expression we use for d_i neglects the ion streaming. The orbit force has a power-law dependence on ion velocity u that assumes superthermal ion flow $u\gg 1$. The expression for the collection force assumes the orbital-motion limited (OML) model of ion collection [25,26] in the same superthermal ion flow limit, $u\gg 1$.

The dust particle's charge z or ''floating potential'' is determined in the steady state by a balance of the electron and ion currents collected by the particle [25,26]. The charging equation for a dust particle is

$$\exp(-z)=\frac{n}{n_e}\sqrt{\frac{\pi m_e}{m_i}}\frac{2z}{\tau}\,\alpha_{\rm ch}, \tag{19}$$

where the left-hand side comes from the electron current (which is suppressed exponentially by electrostatic repulsion), and the right-hand side corresponds to the ion current. In the OML model [25] the ion charging coefficient $\alpha_{\rm ch}$ depends in general on the ion temperature and drift velocity. In the same limit $u\gg 1$ that we used for the collection force,

$$\alpha_{\rm ch}=\frac{1}{\sqrt{\tau}\,u}\left(1+\frac{\tau u^2}{z}\right), \tag{20}$$

so that the ion velocity u will be taken into account in the charging equation.

The dust continuity equation is trivial when the dust is stationary. On the other hand, for a void with moving dust, for example when the void is expanding or contracting in size, the dust continuity equation must be included in the model, so we develop it in Sec. II F.

Now we list the equations for electrons and ions. As in the void, the electrons are Boltzmann distributed,

$$n_e=n_{0e}\exp(\psi).$$

The ion continuity equation in dimensionless units is

$$\frac{\partial nu}{\partial x}=-nP\alpha_{\rm ch}. \tag{21}$$

The right-hand side of Eq. (21) represents absorption on the dust particles. Ionization sources would appear on the right-hand side, but we neglect them in the dust region, as explained earlier. The ion momentum equation is similar to Eq. (9), with the addition of the ion drag force. In dimensionless units it is

$$\frac{\partial(\tau u^2+\psi)}{\partial x}=-zuP\alpha_{\rm dr}. \tag{22}$$

Equations (19), (21), and (22) are used to calculate the left-hand side of Poisson's equation (14) as a linear function of P. Thus Poisson's equation can be solved exactly in the dust cloud to yield an expression for P. The dissipative nature of the dust cloud allows us to find an algebraic solution, without need for numerical methods. The result, which we present as Eq. (A1) in the Appendix, may have wide applications.

F. Dust continuity equation for a moving void boundary

For the case of a void that is expanding or contracting with time, we must pay attention to the moving boundary and find the proper boundary condition for the dust velocity. Let us assume that $x=x_v(t)$ describes the boundary motion, where $x_v(t)$ is the boundary's position at time t. The dust density near the boundary can be written as

$$n_d(x,t)=n_d[x-x_v(t)]. \tag{23}$$

The dust continuity equation for the time-dependent dust distribution is given by

$$\frac{\partial n_d}{\partial t}+\frac{\partial n_d v_d}{\partial x}=0, \tag{24}$$

where n_d and v_d are functions of x and t. Substituting Eq. (23) into Eq. (24), we find

$$\frac{\partial n_d}{\partial x}\left(-\frac{dx_v(t)}{dt}+v_d\right)+n_d\frac{\partial v_d}{\partial x}=0.$$

The dust velocity at the boundary equals the boundary velocity $dx_v(t)/dt$, and

$$\left.\frac{\partial v_d}{\partial x}\right|_{x\to x_v(t)}\to 0. \tag{25}$$

Note that we have assumed a slow motion so that the electrostatic equilibrium is constantly maintained. In this case we are able to investigate the boundary motion, but not the dust motion inside the dust cloud. In dimensionless units, time is normalized as

$$t\equiv\frac{a v_{Tn}}{d_i^2}\frac{n_{0i}}{n_n}\frac{T_e\sqrt{\tau}}{3T_n}t. \tag{26}$$

For the moving void boundary, in the process of matching the electric field, we take the derivative of both sides of Eq. (16). We then use Eqs. (21) and (25) to find $\partial E/\partial x$. This is substituted into Poisson's equation [Eq. (14)].

G. Sharp dust-void boundary

Experiments have shown that the dust-void boundary is a sharp, discontinuous interface [3–5,7,8]. Here we show that in the steady state this is because the force balance acting on dust particles requires a jump in the dust number density at the boundary, provided that the dust kinetic temperature is zero.

First, we must recognize that at the boundary between the dust cloud and the void, the ion and electron parameters, and the electric field, are all continuous. The electric field E is continuous because the particle cloud is a diffuse body that can sustain no surface charge on its boundary. The ion and electron densities and the ion velocity are therefore also continuous. Moreover, the dust charge z is also continuous, since it is determined by the ion and electron parameters.

Second, we generalize the dust force balance Eq. (16) to include a nonzero dust pressure $n_d T_d$. The dust kinetic temperature T_d describes a dust particle's random motion (and should not be confused with the particle's surface temperature, which can be different). In dimensionless units the dust pressure is the product of the dust number density P/z and the dust temperature τ_d, where

$$\tau_d \equiv \frac{T_d e^2}{a T_e^2} = \frac{T_d z}{T_e Z_d}.$$

The generalized force balance for stationary conditions is

$$\tau_d \frac{\partial}{\partial x}\left(\frac{P}{z}\right) = \frac{P}{z}(-zE + nuz^2\alpha_{\mathrm{dr}} - v), \tag{27}$$

where the gradient in the dust pressure appears on the left-hand side. We see that if τ_d is small, then the dust number density P/z has an abrupt jump. Since z is continuous, P also has a jump. Under these conditions, it is valid to use the simplified force balance of Eq. (16), or Eq. (17) for a stationary void.

The jump in P is positive,

$$\Delta P = P_v > 0, \tag{28}$$

since $Z_d > 0$ (negatively charged dust). This jump criterion is necessary to determine whether a void can exist.

The explanation presented above applies to a stationary void. It is also applicable to a void with a moving boundary, provided that the movement is so slow that the force balance is maintained at all times.

We now consider what would happen if one started with a void that had a smooth profile, rather than a sharp edge. As the ions flow from the void into the dust cloud, they are gradually absorbed by the dust. The ion flux will therefore diminish with depth in the dust cloud. Thus the ion drag force will act more weakly on the second dust layer than on the first, and for subsequent layers it will decrease continuously. In other words, the ion drag pressure is most severe on the first dust particles that encounter the ion flow from the void. This pushes the first layer back toward the others, compressing the dust profile so that it develops a sharp edge.

There are several effects which could cause the jump in dust density to become a smooth profile rather than a sharp jump. These effects are finite dust particle temperature, finite particle size dispersion, and finite dust particle inertia. If the dust temperature is not small, $T_d \ll T_e Z_d/z$, then the left-hand side of Eq. (27) is not negligible and the jump is continuous. If the particle size distribution is not monodisperse, then particles will separate at the boundary according to size. This will occur because two forces on the right-hand side of Eq. (27) scale differently with particle size. The electric force is $\propto a$, whereas the ion drag force is $\propto a^2$. Particle inertia would appear as an additional term, with the particle mass and a convective derivative of v on the left-hand side of Eq. (27). As long as the particle mass is small enough (typically $\ll 2$ μm), or, alternatively, as long as the problem is nearly steady state $\partial/\partial t = 0$ and stationary $v = 0$, inertia effects will be negligible.

H. Equations and boundary conditions for numerical solution

The numerical results we will present are valid in the void region $x \leqslant x_v$. The equations for the dust region $x \geqslant x_v$ are used primarily to provide boundary conditions at x_v, and to establish whether a void can exist. The equations in the void region form a simple set of the first order differential equations. We have

$$\frac{d\psi}{dx} = -E \tag{29}$$

and

$$\frac{\partial E}{\partial x} = -\left(\frac{d_i}{a}\right)^2\left(\exp(\psi) - \frac{x}{\sqrt{-\psi}\,x_{0i}}\right). \tag{30}$$

Solutions of Eqs. (29) and (30) should satisfy two boundary conditions at the dust cloud boundary, namely, the continuity of the electric field and the dust charging equation (19). These will yield the position of the void's boundary x_v and the dust particle charge z_v at the boundary. From Eqs. (10), (17), and (18), we have the force balance equation

$$E(x_v) - \frac{\sqrt{\tau}\, z_v x_v}{2x_{0i}[-\psi(x_v)]^{3/2}}\left\{\ln\left(\frac{d_i}{a}\right) - \frac{\psi(x_v)}{z_v} + \frac{[\psi(x_v)]^2}{z^2}\right\} = 0, \tag{31}$$

and from Eqs. (10), (19), and (20) we find the charging equation

$$\exp[-z_v + \psi(x_v)] = \sqrt{\frac{\pi m_e}{2m_i}}\frac{x_v/x_{0i}}{\sqrt{-\psi(x_v)}}\left[\frac{z_v}{\sqrt{-\psi(x_v)}} + \frac{\sqrt{-\psi(x_v)}}{2}\right]. \tag{32}$$

On the left-hand side the sum of the floating potential and plasma potential, $-z_v + \psi(x_v)$, is essentially the floating potential of a particle at the void's boundary with respect to the potential at the void's center.

Equations (31) and (32) should be solved together with the jump criterion [Eq. (28)], which is the consequence of the analytical solution in the dust region. At the boundary, we have the exact solution

$$P_v = \frac{x_v[-\psi(x_v)]^{-1/2} - e^{\psi(x_v)} + 8^{-1}\tau a^2 z_v^2 x_v^2 [\psi(x_v)]^{-4} A_n(\sqrt{-2\psi(x_v)})}{1 + 8^{-1}\tau a^2 x_v[-\psi(x_v)]^{-7/2} B_n(\sqrt{-2\psi(x_v)})}, \tag{33}$$

where coefficients A_n and B_n are given by Eqs. (A3) and (A4) in the Appendix.

For each run of calculations, Poisson's equation (30) in the void region is solved numerically to determine the electric field $E(x)$. This integration is not begun at $x=0$, where there would be nonphysical accumulations of ion charge due to $u_i=0$ there. Instead we assume Eq. (13) for $x \ll x_v$ and begin the integration at a finite value of x. Once we have $E(x)$, we next find $\psi(x)$ using Eq. (29), and $u(x)$ using Eq. (10).

The boundary conditions at the void boundary $x=x_v$ are the following: continuity of E, u, and ψ at the boundary; the force balance equation (31); the charging equation (32) at the boundary; and the jump condition. The latter condition, expressed in Eqs. (28) and (33), is a test that determines whether an equilibrium void can exist.

III. NUMERICAL RESULTS

A. Stationary voids

Numerical results valid inside a void in a dusty argon plasma are presented in Fig. 5. These show the structure of the potential $\psi(x)$, ion velocity $M(x)$, and electric field $E(x)$ in the void. The parameters are dimensionless dust size $a=0.01$ (corresponding typically to micron-size particles), $T_i/T_e=0.05$, and a dimensionless ionization rate $1/x_{0i}=0.15$. The solutions are presented beginning at $x=1.3$ where the integration began. The void's edge is marked in these profiles; its location was found from the boundary conditions.

The ions flow from the void center toward the edge. They accelerate toward the void boundary. The ions attain a speed almost exactly equal to the ion acoustic speed, i.e., a Mach number of unity, when they reach the boundary. This condition is analogous to the Bohm criterion for a collisionless sheath. The ions are subsonic in the void and sonic as they enter the dust cloud. This result validates the assumption of superthermal ions used in Eq. (18) in the void region.

The potential in Fig. 5(a) varies smoothly, with a nearly parabolic dependence on x in most of the void. There are small oscillations superimposed on the otherwise smooth monotonic shape of the potential profile. These oscillations are also apparent in the ion velocity in Fig. 5(a), but they are most prominent in the electric field [Fig. 5(c)]. These spatial oscillations reveal the presence of a stationary ionization striation. In a test, we verified that they are suppressed when ion-neutral collisions are included in the model. The only conditions where these oscillations pose a problem in our solutions are when the potential fluctuates to a positive value, so that a solution cannot be found. This problem is generally avoided by starting the numerical integration at a sufficiently large x.

Near the void edge, the potential and the electric field vary rapidly with x. This occurs beyond the point where the oscillatory regime dies out, e.g., for $x>2.8$ in Fig. 5.

We varied the ionization rate $1/x_{0i}$ to find the parameters where a void can exist, and the dependence of the void size on ionization rate. The results are shown in Fig. 6. We fixed the other parameters, including dust size $a=0.01$, $T_i/T_e=0.05$, and argon ions. At the extreme of high ionization rate, we stopped our parameter scan in Fig. 6 when the void became too small for our method of integration, which began at a finite value $x=1.3$.

There are intermittent regions of parameter space where we found no equilibrium void solutions. These are shown in Fig. 6 with shaded boxes. We cannot be certain whether the limitations of our numerical solvers account for these regions of no solution, or whether there is truly no physical solution there. In any case, one would expect that, below a minimum ionization rate, there will not be enough outward ion drag force to maintain the void. Examining Fig. 6, the minimum ionization rate is the first data point on the left.

As the ionization rate increases, it generally follows the scaling $x_v \propto x_{0i}$. This power-law scaling is easily seen as a constant slope in the log-log plot in Fig. 6. The trend of void size diminishing with ionization rate $1/x_{0i}$ is consistent with having an ion velocity in the intermediate regime for ion drag shown in Fig. 3. In the collisionless case, the ion velocity increases continuously with distance from the void center, as shown in Fig. 5. This means that the ion drag force diminishes as the ions flow outward. A force balance is attained when the ion drag force finally becomes as weak as the electrostatic force. This determines the size of the void. A higher ionization rate causes a higher potential to develop between the void and the dust, accelerating the ions to a higher ion velocity in a shorter distance, thereby yielding a smaller void.

This inverse dependence of the void size and ionization rate should be compared to the experimental results. Both Samsonov and Goree [4] and Morfill *et al.* [8] found that the void size increased when the rf power that sustained the discharge was increased. Recall that the ionization rate increases exponentially with T_e. Our results are consistent with the experiments only if T_e decreases with the applied rf power, but it is not known from the experiments whether this is true. If there is a disagreement between our result and the experiment, there are two possible explanations. First, it is possible that there truly is a solution to our equations that our numerical solvers failed to find in the leftmost shaded region of Fig. 6, and that this solution has a void size that increases with ionization rate. Second, we have neglected ion-neutral collisions, which would reduce the ion velocity. We have not

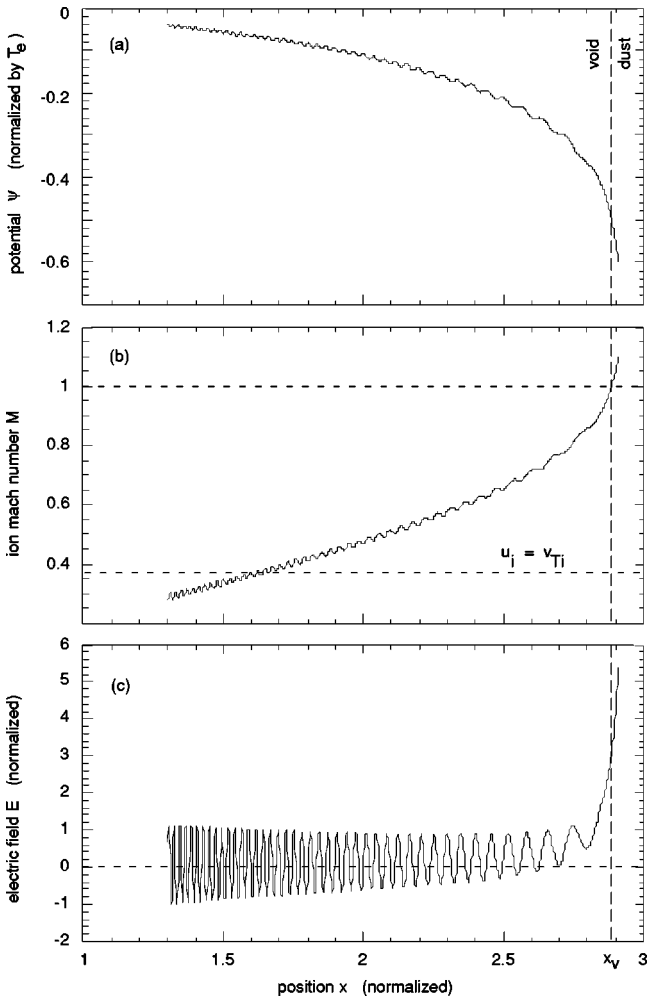

FIG. 5. Solutions in the void region showing the spatial profiles of (a) the normalized electrostatic potential ψ, (b) the normalized electric field E, and (c) the Mach number of the ion flow. Parameters assumed were $a=0.01$, $T_i/T_e=0.05$, and $1/x_{0i}=0.15$ in an argon plasma. The origin at $x=0$ is suppressed in this plot. The void edge, determined from the boundary conditions, was found to be $x_v=2.876$. Note that the ion Mach number is almost exactly unity at the void edge. The ion thermal velocity indicated by a dashed line in (b) has a Mach number of 0.376.

solved the latter problem, so we are unable to say whether this could lead to a void size that increases with ionization rate.

For all the stable void solutions in our parameter scan of Fig. 6, we found that the Mach number of the ion flow was almost exactly unity at the boundary. This is analogous to the Bohm criterion of a collisionless sheath, except that there is nothing like an electrode in our model of the dust cloud. In a collisionless sheath, the ion velocity is subsonic in the main plasma and becomes supersonic in the sheath. Ions then flow through the sheath to the electrode. Drawing on a sheath analogy, we would say that the ''sheath'' in a void-dust cloud system is localized inside the dust cloud rather than in the void. Indeed, the numerical solutions of Ref. [27] showed that the electric potential drop occurs mostly inside the dust cloud.

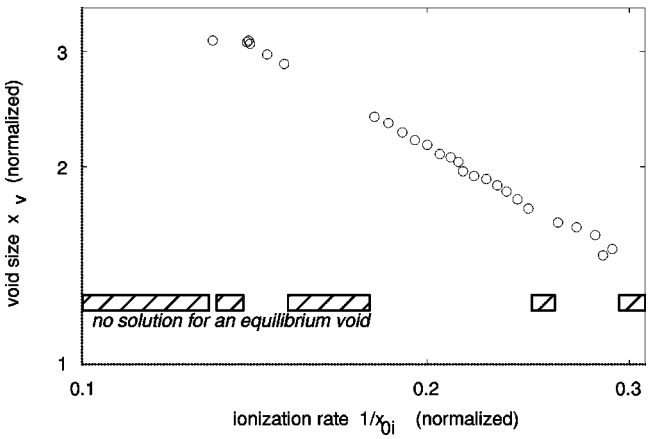

FIG. 6. Dependence of the void size x_v on the ionization rate $1/x_{0i}$ within the range $0.1<1/x_{0i}<0.3$. Regions where no equilibrium solution exist are shown with shaded boxes. There are no equilibrium solutions for $1/x_{0i}<0.1$ because the ionization rate is too low to produce an outward ion flux adequate to sustain the void.

B. Voids that expand or contract with time

By including a moving boundary between the void and dust cloud, but keeping the void center stationary at $x=0$, we modeled the problem of a void that can expand or contract with time. The motion must be slow enough that the equilibrium force balance on dust particles is always maintained. Under these conditions it is still possible to find the velocity of the void's edge, because the force balance includes the dust-neutral drag force, which depends on the dust velocity.

Results are shown in Fig. 7. The parameters assumed here are a relatively large dust size $a=0.1$ and a low ionization rate $1/x_{0i}=0.09$.

The phase diagram shown in Fig. 7(a) is a plot of velocity vs position of the void edge x_v. This phase diagram reveals a single stable equilibrium void size, where the velocity of the void edge dx_v/dt is zero. Smaller voids will grow, because their edge will have a positive velocity. Larger voids will shrink, with an edge moving with a negative velocity. This ''stationary point'' feature of the phase diagram was found for all the parameters we tested. It indicates a single stable equilibrium for a given particle size and ionization rate. This is a noteworthy result that we compare to experimental results in Sec. IV.

Contracting voids with a size larger than a maximum cannot exist. This maximum size should not be confused with the maximum size of a stationary void, as in Sec. III A (that maximum size corresponds to a minimum ionization rate for sustaining the void). Here we refer to the maximum size of a void that is contracting toward its stationary size. Near the maximum size, the velocity of the void's edge is always directed inwards, i.e., the void is contracting. The maximum possible void size for all investigated cases was larger than the size of a stationary void.

The dust charge in Fig. 7(b) has a maximum for a void size slightly larger than the stationary void size. The charge decreases rapidly for voids that are large and shrinking, i.e., near the maximum void size.

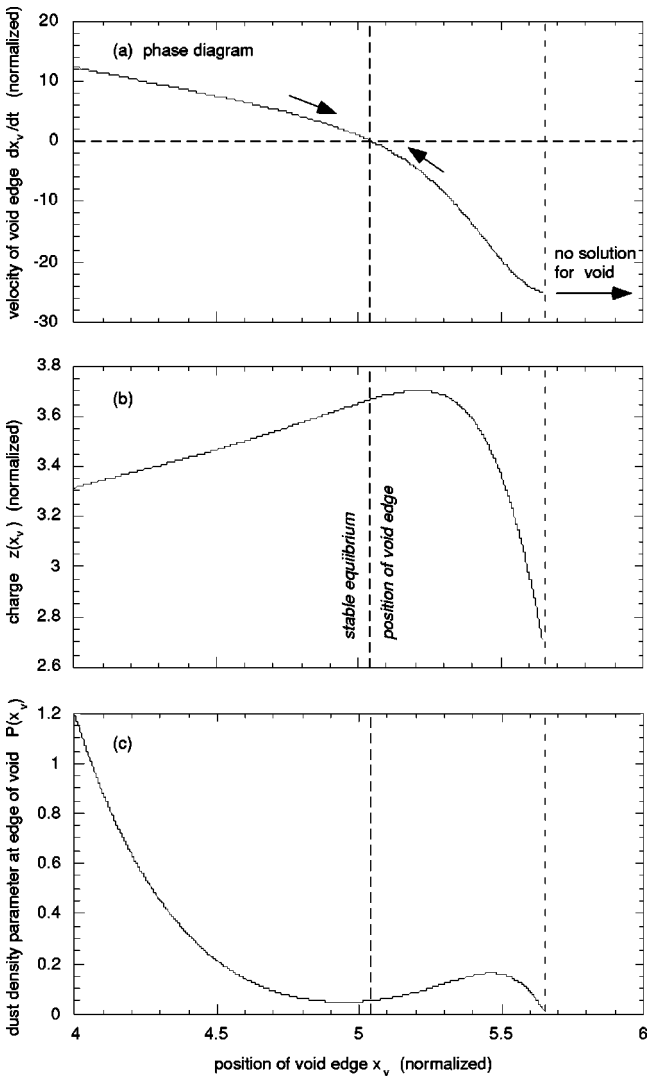

FIG. 7. Solutions for an expanding or contracting void, showing the spatial profiles of (a) the normalized velocity of the void edge dx_v/dt, (b) the normalized dust charge z at the void edge, and (c) the jump of the dust number density parameter P at the void edge. Parameters assumed were $a=0.1$, $T_i/T_e=0.05$, and $1/x_{0i}=0.09$ in an argon plasma. The phase diagram (a) shows a stationary point. Larger voids contract and smaller voids expand. There is a maximum size for a contracting void; it occurs where the dust density jump becomes zero.

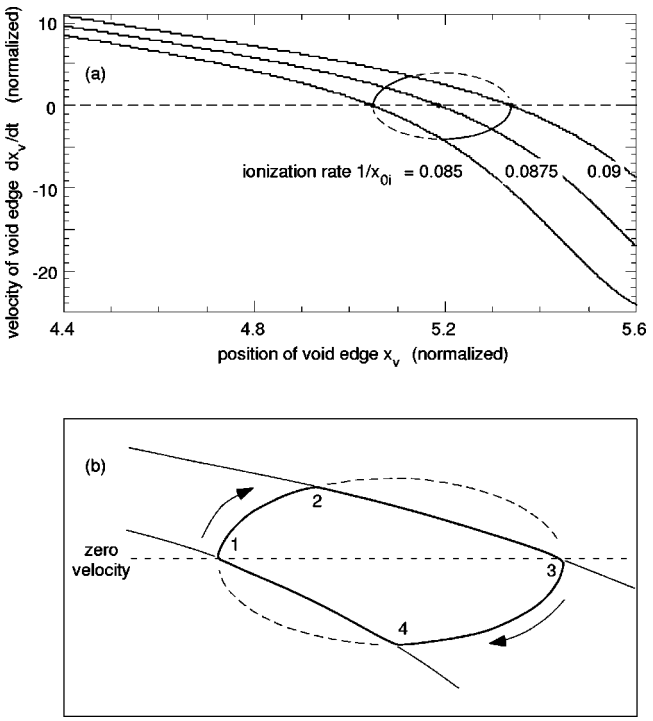

FIG. 8. Phase diagrams. (a) As in Fig. 7(a), but with two additional curves for different ionization rates. The equilibrium size of the void, indicated by the stationary point, depends on the ionization rate. (b) Sketch of the evolution of the system if the ionization rate is changed in steps $1-2$ and $3-4$. Magnified compared to (a). The void size expands and contracts in the cycle steps $1-2-3-4-1$.

We repeated these calculations for a wide range of dust size and ionization rate. The equilibrium void size, i.e., the stationary point on the phase diagram, depends sensitively on the ionization rate. This is shown in Fig. 8(a), where the phase diagram curves cross zero at different void sizes, depending on the ionization rate. Other results, stated briefly, were as follows. For smaller dust particles and larger ionization rates, the contracting velocity can be very large while the expanding velocities are low. In this case, the dust density jump P_v for a contracting void has a large maximum value while an expanding void has a smaller jump. For larger dust sizes and smaller ionization rates, the dust density jump is much larger for expanding voids than that for the contracting void. In this case expanding voids have velocities comparable to, or lower than, contracting voids. For all cases the expansions or contractions finish at a stationary void size.

C. Global void stability

For a stable void to exist, the particle size and ionization rate parameters must allow a stable equilibrium. This occurs for some parameters but not all, as shown in Sec. III A. This condition is not sufficient, however. In addition to having a stable stationary size, the moving size must not be too large, as shown in Sec. II B.

The reason voids larger than the maximum moving size cannot exist is that the dust particle charge would be too small to allow a force balance. In Fig. 7(c) the dust number density parameter P at the void edge diminishes rapidly near the maximum void size.

A void that is expanding or contracting will not oscillate about the stationary equilibrium size, but rather will approach it asymptotically. This is shown in the time series of Fig. 9, which corresponds to the phase diagram in Fig. 7(a). The time required for the expanding or contracting void to approach is typically about unity in our dimensionless units. Using the normalization for time [Eq. (26)], this formation time in physical units is

$$t_v \approx \frac{d_i^2}{a v_{Tn}} \frac{3T_n}{T_e\sqrt{\tau}} \frac{n_n}{n_{0i}}. \tag{34}$$

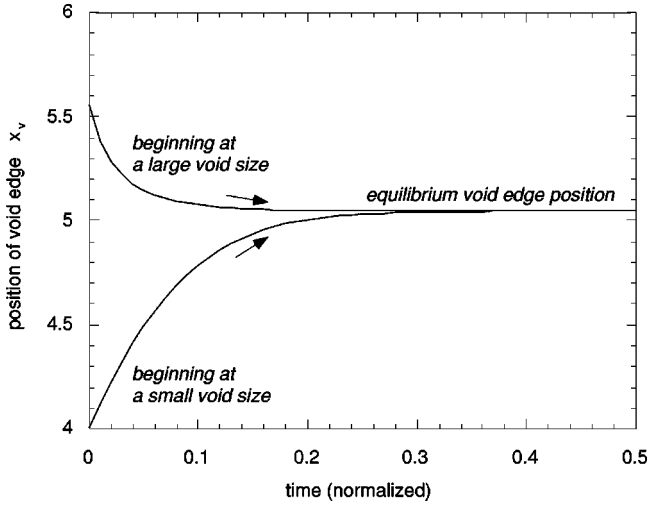

FIG. 9. Temporal evolution of the void size. These data correspond to the phase diagram of Fig. 7(a), with the same parameters. The upper and lower curves show the evolution of a void with an initial size larger and smaller than the stationary void size, respectively. The void size asymptotically approaches the stationary void size. Time here is normalized as in Eq. (26).

The characteristic time τ_v in Eq. (34) is of the order 0.1 sec for typical experimental parameters: $d_i^2/a \approx 100$ μm, $v_{Tn} \approx 3\times 10^4$ cm/s, and an ionization fraction $n_{0i}/n_n \approx 10^{-7}$–$10^{-6}$ in argon gas.

D. Oscillation of void size

While the void in the experiment of Morfill *et al.* [8] was usually stable, under some operating conditions it underwent a 1.5-Hz relaxation oscillation. This mode was termed the ''heartbeat'' because the particles underwent a throbbing motion like a muscle in a heart. The void repeatedly collapsed to a no-void condition, and then returned to the original size. In phase space, this corresponds to a cycle rather than a stationary point.

The experiment flew on a sounding rocket to provide microgravity conditions. This allowed the entire plasma volume to be filled with dust in a way that would be possible in the laboratory only by using smaller particles. The rf generator applied a sinusoidal voltage at the fundamental frequency, and the forward power was regulated as a constant. The voltage and current were not regulated, but at the fundamental frequency 13.5 MHz they were observed to remain constant during the heartbeat. However, the harmonics of the rf on the electrode were observed to be modulated at 1.5 Hz. These harmonics are generated by the nonlinear impedance of the plasma. The modulation of the harmonics indicates that some internal plasma parameter varied with the void size.

It is unknown exactly which internal parameters were modulated. Here we will speculate how the ionization rate, if it was modulated with the void size, could explain the cyclical variation of the void size.

The model we have presented includes a fixed ionization rate. This is equivalent to assuming a uniform and constant T_e. Because of this assumption, the model is unable to predict the phase diagram quantitatively if the ionization rate in a gas discharge varies self-consistently as the void size expands or contracts. However, we can make a qualitative prediction. We do this using the phase space diagram in Fig. 8(a), to determine the evolution of the void size if the ionization rate is changed as an external parameter. This is sketched in Fig. 8(b). We begin at point 1, and then increase the ionization rate (by increasing T_e for example), doing this fast enough ($t \ll 1$) that the system does not follow an isoionization-rate curve. The void size then expands from the stationary point of one isoionization-rate curve to another, $1 \rightarrow 2$. Then we fix the ionization rate, and the void size expands further along isoionization-rate curve $2 \rightarrow 3$, until it reaches a new stationary point 3. Then we decrease the ionization rate back to the original rate, so that the void contracts rapidly $3 \rightarrow 4$ and then $4 \rightarrow 1$. This completes our cycle. It illustrates how an ionization rate that varies with void size can lead to a cycle similar to that observed in the experiment of Morfill *et al.* It is idealized, and not an exact simulation of the experiment.

IV. CONCLUSIONS

We have demonstrated that a void is a stable equilibrium in a dusty plasma when there is sufficient ionization. The void is maintained by a balance of an outward ion drag force and an inward electrostatic force.

We developed one-dimensional nonlinear fluid equations for both the void and dust cloud regions. These include dust charging, ion drag forces on dust, and an ionization source. We solved them numerically in the void region, and applied boundary conditions at the void's edge, based on the equations in the dust region.

The approximations, particularly our assumption of collisionless ions, limit the model's ability to make quantitative predictions for the experiments, which are always conducted with significant ion-neutral collisions. Nevertheless, many of the qualitative features of our results are suitable for comparison to the experiments.

One of our results that agrees with all the reported experiments is the existence of a sharp edge at the boundary between the void and the surrounding dust cloud. We found that this is due to the force balance on a dust particle. Provided that the dust has a zero kinetic temperature and the particles have a uniform size, the force balance can be satisfied only if there is a discontinuity in the dust number density. There is no discontinuity, however, in the potential, electric field, ion velocity, or other plasma parameters.

There is always either a single stable equilibrium size for the void, or there is no void at all. In a phase diagram, there was a single stationary point, if there was any solution at all, for a fixed ionization rate. When a void is expanding our contracting with time, we find that it always asymptotically approaches the equilibrium stationary size. It does this without any oscillations, provided that the ionization rate is held constant, and it achieves the final equilibrium size fairly rapidly, on a time scale of about 0.1 sec in the experiments. On the other hand, if the ionization rate in the void varies in time in some self-consistent manner with the void size and other plasma parameters, it is possible for the void size to oscillate in a repetitive cycle as was observed in the microgravity experiment of Morfill *et al.* [8].

Our problem resembles in many ways a collisionless sheath problem. The outward-flowing ions attain a Mach number of unity when they arrive at the void edge. We did not attempt to continue our numerical solutions into the dust cloud, although this was done by Tsytovich, Benkadda, and Vladimirov [27], who neglected ionization but included a second boundary on the other side of the dust cloud. The dust cloud contains the region analogous to a sheath, where the electric potential has its drop.

The experimental results of Samsonov and Goree [4] and Morfill *et al.* [8] indicated that the void size increased when the rf power that sustained the discharge was increased. In our model, the void size decreases with the ionization rate, and therefore decreases with T_e. We do not know whether this result is consistent with the experimental result, since there were no measurements of T_e vs rf power made in the experiments.

One way the model could be improved so that it can be compared more directly to the experiments is by including ion-neutral collisions. These would reduce the ion velocity, which in turn would affect the ion drag force, the dust charge, and the electric field at the void boundary. One possible approach to including ion-neutral collisions would be to assume mobility-limited ion motion. In a noble gas, the ion velocity scales $\propto E/N$ for low values of E/N, where N is the neutral gas pressure, but $\propto (E/N)^{1/2}$ for higher values [28]. The transition between these two regimes occurs at the ion thermal velocity, which coincidentally is where the ion drag force undergoes a transition, as shown in Fig. 3.

ACKNOWLEDGMENTS

Author J.G. was supported in part by NASA and the National Science Foundation. V.N.T. was sponsored at the Max Planck Institut für Extraterrestrische Physik by an A. von Humboldt award. S.V.V. was partially supported by the Australian Academy of Sciences and the Australian Research Council.

APPENDIX: EXPRESSION FOR DUST DENSITY PARAMETER P IN THE DUST REGION

An expression for the dust density parameter P is found by substituting Eq. (16) into Eq. (14) and using Eqs. (20) and (21). The result is

$$P=\frac{d_i^2(n-n_e)+\tau a^2[A_w(M)w^2+A_{wn}wn+A_n(M)n^2]}{d_i^2+\tau a^2[B_w(M)w+B_n(M)n]}, \tag{A1}$$

where $w=v/\tau$, v is the dust velocity with respect to the neutral gas background, and M is the Mach number of the ion flow, which at the dust boundary is equal to its value in the void

$$M^2=2\tau u^2=-2\psi. \tag{A2}$$

The coefficients A and B in Eq. (A1) are

$$A_w(M)=-\frac{1}{z^2M^2}\frac{2M^2z+M^4-4z}{2z^2+2z+M^2z},$$

$$A_{wn}(M)=-\frac{1}{M^4}\left[\Lambda(M)\frac{2z^2+6z-M^2z-M^4}{2z^2+2z+M^2}+\Lambda_*(M)\frac{4z^2+4M^2z+M^4}{2z^2+2z+M^2}\right], \tag{A3}$$

$$A_n(M)=\frac{z^2\Lambda(M)}{M^6}\left[\Lambda(M)+\Lambda_*(M)\frac{4z^2+4M^2z+M^4}{2z^2+2z+M^2}\right],$$

$$B_w(M)=\frac{1}{zM^4}\left[\frac{M^2}{2z}\left(1+\frac{M^2}{2z}\right)^2-2\Lambda(M)\right]\frac{2z}{2z+2+M^2},$$

$$B_n(M)=\frac{z^2}{M^6}\left[\Lambda^2(M)+2\Lambda(M)\Lambda_*(M)\frac{2z+M^2}{2z+2+M^2}+\frac{M^2}{2z}\left(1+\frac{M^2}{2z}\right)\left(\Lambda_*(M)\frac{2z+M^2}{2z^2+2z+M^2z}-\Lambda(M)\right)\right], \tag{A4}$$

where

$$\Lambda(M)=\ln\left(\frac{d_i}{a}\right)+\frac{M^2}{2z}+\frac{M^4}{4z^2},\quad \Lambda_*(M)=\ln\left(\frac{d_i}{a}\right)-\frac{M^4}{4z^2}.$$

Equation (A1) is a generally useful result for the dust density parameter in a plasma, in the absence of ion-neutral collisions. In the main paper we use it for a specialized purpose, evaluating it only at the boundary of the void, $x=x_v$.

All the expressions above assume equilibrium condition $\partial/\partial t=0$. This allows for the possibility that either the dust is stationary, or that it moves so slowly that the dust inertia is insignificant and equilibrium conditions are maintained at every moment.

[1] A. Garscadden, B. N. Ganguly, P. D. Haalard, and J. Williams, Plasma Sources Sci. Technol. **3**, 239 (1994).
[2] V.N. Tsytovich, Usp. Fiz. Nauk **167**, 57 (1997) [Phys. Usp. **40**, 53 (1997)].
[3] G. Praburam and J. Goree, Phys. Plasmas **3**, 1212 (1996).
[4] D. Samsonov and J. Goree, Phys. Rev. E **59**, 1047 (1999).
[5] D. Samsonov and J. Goree, IEEE Trans. Plasma Sci. (to be published).
[6] D. Samsonov and J. Goree, video of an ionization instability in a dusty plasma, http://dusty.physics.uiowa.edu/Movies/Movie/index.html.
[7] A. Melzer, A. Piel, and V. Schweigert (unpublished).
[8] G. E. Morfill, H. M. Thomas, U. Konopka, H. Rothermel, and M. Zuzic (unpublished).
[9] O. Havnes, T. Aslaksen, and F. Melandsø, J. Geophys. Res. **95**, 6581 (1990).
[10] M. Barnes, J. H. Keller, J. C. Forster, J. A. O'Neil, and D. K. Coultas, Phys. Rev. Lett. **68**, 313 (1992).
[11] G. S. Selwyn *et al.*, Plasma Sources Sci. Technol. **3**, 340 (1994).
[12] O. Havnes, U. de Angelis, R. Bingham, C. K. Goertz, G. E. Morfill, and V. N. Tsytovich, J. Atmos. Terr. Phys. **52**, 637 (1990).
[13] N. N. Gor'kavyi and A. M. Fridman, *Fizika Planetarnykh Kolets (Physics of Planetary Rings)* (Nauka, Moscow, 1994).
[14] V. N. Tsytovich Aust. J. Phys. **51**, 763 (1998).
[15] V. N. Tsytovich (unpublished).
[16] In Ref. [14] it was shown that at the edge of a dust cloud, with local quasineutrality, there is a jump in the derivative of the dust density, but not the dust density itself, although outside the dust cloud the dust density is zero and the edge is not diffusive. Subsequently, in Ref. [15] it was shown that if quasineutrality inside the cloud is violated, both the dust density and its derivative should have jumps at the boundary. In both cases, ionization was neglected, so that the problem treated was the converse of a void.
[17] N. D'Angelo, Phys. Plasmas **5**, 3155 (1998).
[18] T. E. Sheridan and J. Goree, IEEE Trans. Plasma Sci. **17**, 884 (1989).
[19] T. E. Sheridan and J. Goree, Phys. Fluids B **3**, 2796 (1991).
[20] M. D. Kilgore, J. E. Daugherty, R. K. Porteous, and D. B. Graves, J. Appl. Phys. **73**, 7195 (1993).
[21] J. Boeuf, Phys. Rev. A **46**, 7910 (1992).
[22] M. A. Lieberman and A. J. Lichtenberg, *Principles of Plasma Discharges and Materials Processing* (Wiley, New York, 1994), pp. 454–460.
[23] P. Epstein, Phys. Rev. **23**, 710 (1924).
[24] M. J. Baines, I. P. Williams, and A. S. Asebemio, Mon. Not. R. Astron. Soc. **130**, 63 (1965).
[25] E. C. Whipple, Rep. Prog. Phys. **44**, 1198 (1981).
[26] J. Goree, Plasma Sources Sci. Technol. **3**, 400 (1994).
[27] V. N. Tsytovich, S. Benkadda, and S. V. Vladimirov, Czech J. Phys. **48**, Suppl. 2, 71 (1998).
[28] L. S. Frost, Phys. Rev. **105**, 354 (1957).